Physics and Imaging in Radiation Oncology 32 (2024) 100681

Contents lists available at ScienceDirect

Physics and Imaging in Radiation Oncology

journal homepage: www.sciencedirect.com/journal/physics-and-imaging-in-radiation-oncology

Original Research Article

Feasibility and potential clinical benefit of dose de-escalation in stereotactic ablative radiotherapy for lung cancer lesions with ground glass opacities

Carla Cases [a,*], Meritxell Mollà [a,b,c,d], Marcelo Sánchez [d,e], Mariana Benegas [d,e], Marc Ballestero [a], Sergi Serrano-Rueda [a], Gabriela Antelo [a,d], Carles Gomà [a,b]

[a] Department of Radiation Oncology, Hospital Clínic, Barcelona Spain
[b] Translational Genomics and Targeted Therapies in Solid Tumors, Institute for Biomedical Research August Pi i Sunyer (IDIBAPS), Barcelona, Spain
[c] Department of Clinical Foundations, University of Barcelona, Barcelona Spain
[d] Thoracic Oncology Unit, Hospital Clínic, Barcelona Spain
[e] Department of Radiology, Hospital Clínic, Barcelona Spain

A B S T R A C T

Introduction: Treatment of neoplasic lung nodules with ground glass opacities (GGO) faces two primary challenges. First, the standard practice of treating GGOs as solid nodules, which effectively controls the tumor locally, but might increase associated toxicities. The second is the potential for dose calculation errors related to increased heterogeneity. This study addresses the optimization of a dose de-escalation regime for stereotactic ablative radiotherapy (SABR) for GGO lesions.
Materials and Methods: We used the CT scans of 35 patients (40 lesions) with some degree of GGO component treated at our institution between 2017 and 2021. We first assessed the dose calculation accuracy as a function of the GGO component of the lesion. We then analysed the advantages of a dose de-escalation regime in terms of lung dose reduction (Dmean, V20Gy and V300GyBED3) and plan robustness.
Results: We found a positive correlation between the presence of GGO and the dose calculation errors in a phantom scenario. These differences are reduced for patient data and in the presence of breathing motion. When using a de-escalation regime, significant reductions were achieved in mean lung dose, V20Gy and V300GyBED3. This study also revealed that lower doses in GGO areas lead to more stable fluence patterns, increasing treatment robustness.
Conclusions: The study lays the foundation for an eventual use of dose de-escalation in SABR for treating lung lesions with GGO, potentially leading to equivalent local control while reducing associated toxicities. These findings lay the groundwork for future clinical trials.

1. Introduction

Lung stereotactic ablative radiotherapy (SABR) has proven to be an effective treatment for inoperable lesions, offering good local control (LC) and a low incidence of grade ≥ II toxicities [1–4]. Most lung SABR treatments target solid pulmonary nodules. However, an increasing percentage are administered to nodules with some component of ground-glass opacity (GGO). These opacities are present in minimally invasive adenocarcinomas, lepidic-predominant adenocarcinomas, and invasive mucinous adenocarcinomas and exhibit a more indolent clinical course [5–8]. Furthermore, the GGO component is considered to correspond to a non-invasive histology, while the solid component is considered as the invasive part of the lesion [9]. Nonetheless, with the widespread use of screening [10], small-sized pulmonary nodules, especially those containing GGO component, are increasingly detected [11].

Over the years, several SABR regimes have been used to treat lung lesions. Some studies have analyzed different SABR regimes in terms of biologically effective dose (BED) and its relation to local control [12] and/or clinical toxicity [4,13,14]. Over the last years, lower BED regimes have been prioritized to reduce toxicities. However, it has been reported that lowering the prescribed BED below the threshold of 100 Gy_{BED10} (where the subscript 10 refers to the alpha/beta ratio considered for calculation) comes at the cost of lower LC rates [15,16].

In this context, which sets a lower threshold to grant acceptable LC rates, and an upper threshold to reduce associated toxicities, some groups have studied the use of different dose levels within the lesion for specific cases. Dose de-escalation has been proposed to avoid chest wall toxicity, while maintaining LC rates [17]. Conversely, others have analyzed the outcomes of using a simultaneously integrated boost for larger lesions [18] achieving promising LC rates.

The SABR treatment of GGO faces two primary challenges. The first is the standard practice of treating GGO as solid nodules. This approach is problematic when treating a small solid component within a larger GGO, as the risk of lung toxicity correlates with the volume of lung receiving a high dose [19]. While this strategy effectively controls the

* Corresponding author.
E-mail address: cases@clinic.cat (C. Cases).

https://doi.org/10.1016/j.phro.2024.100681
Received 24 April 2024; Received in revised form 20 November 2024; Accepted 20 November 2024
Available online 29 November 2024

tumor locally [20], it increases the risk of damaging healthy lung tissue to a lesion expected to have better LC rates [21]. Tailoring SABR treatments for this kind of lesion seems advisable, as GGO tumors are often multifocal and may require multiple subsequent irradiations.

The second challenge involves the potential for large dose calculation errors by commercial dose calculation algorithms, owing to the increased heterogeneity of GGO lesions [22–24]. To our knowledge, no studies have yet evaluated the dose calculation errors in GGO lesions. Furthermore, challenges related to fluence peaks during optimization should be considered, as they lead to less robust dose distributions [25]. This effect is especially significant when optimizing with type C algorithms and several approaches have been presented for solid lesions [26,27]. With all the aspects in mind, optimizing SABR treatment for GGO malignancies is an essential step to ensure the best treatment option for these malignancies, which are expected to be increasingly diagnosed.

In this study we focus on analyzing the feasibility of performing a dose de-escalation that ensures dose calculation accuracy and robustness. We propose a method to efficiently implement dose de-escalation for lung lesions containing varying amounts of GGO component and report the expected differences in lung dose, robustness, and dose accuracy compared to the standard approach of a single dose level.

2. Materials and methods

To assess the technical feasibility of dose de-escalation, we used two datasets. First, we analyzed dose calculations performed on the CT scan of a thoracic static anthropomorphic phantom (IMRT Thorax phantom, CIRS, SUN Nuclear, Norfolk). Second, we evaluated the dose calculation accuracy, dose reduction achieved, and the robustness of the plan on the CT scans of 40 lesions (from 35 patients) treated at our institution between 2017 and 2021, which exhibited some component of GGO in the lesion.

To describe the amount of GGO present in the lesion, we used the consolidation to tumor ratio (CTR), defined as the diameter of the solid part of the lesion divided by the total diameter [28]. In this study, we have also included the volumetric CTR (CTR_v), defined as the volume of the solid component divided by the total lesion volume.

Our patients were originally treated following the Radiation Therapy Oncology Group (RTOG) 0236 trial protocol and the giudelines included in the clinical study approved by the ethics board at our institution. We prescribed two fractionation schemes, depending on the size, centrality, and proximity of the tumor to organs at risk. The schemes consisted of 3 fractions of 18 Gy or 5 fractions of 11 Gy. The radiation oncologist defined the internal target volume (ITV) using the 10 phases of the 4DCT, as it allowed a better differentiation of the solid and GGO component. An isotropic margin of 3 mm was added to the ITV to define the planning target volume (PTV). We optimized the treatment using volumetric modulated arc therapy (VMAT), with a dose normalization ensuring that the 100 % isodose level encompassed 95 % of the PTV.

The BED of the two considered fractionation schemes for the GTV are 115 Gy $_{BED10}$, and 151 Gy $_{BED10}$ for the 5, and 3 fractions case, respectively. Our dose de-escalation strategy was to lower the dose to the GGO component of the PTV to 100 Gy_{BED10}, while maintaining the dose to the solid part as per the original prescription, thus reducing the prescribed dose to the GGO component to 10 Gy and 14 Gy for the 5 and 3 fraction case respectively.

2.1. Evaluation of dose calculation accuracy as a function of GGO component

To evaluate the dosimetric impact of the algorithm used, we first used the CT scan of the thoracic phantom. We contoured a set of spherical lesions in the lung region with diameters of 10, 15, 20, 30, and 40 mm; and CTRs of 0, 0.25, 0.50, 0.75 and 1 for every diameter. We manually assigned a physical material value to each region inside the PTV: water (1 g/cm^3) for the solid kernel and lung (0.6134 g/cm^3) for the GGO shell (Fig. 1). Regarding the clinical cases, we studied two scenarios: (i) the average reconstruction of a 4DCT scan simulating an ITV approach, and (ii) the 50 % expiration phase of the 4DCT scan, to simulate the results in the case of a gated treatment, which could further improve the dose reduction [32]. The solid component and the GGO component were delimited in each phase of the CT scan, and a solid ITV (ITVs) and a GGO ITV (ITVGGO) were defined. Their corresponding PTVs were also defined by adding a 3 mm margin to their corresponding ITV.

To evaluate dose inaccuracies in both datasets, we calculated (Eclipse v16.0) VMAT treatment plans with a dose prescription of 55 Gy in 5 fractions. We optimized and calculated the dose distribution using AAA and then recalculated these plans using $AXB_{m,m}$ (m,m indicates transport in medium, dose to medium) with fixed monitor units (MU). Optimization was performed with heterogeneity corrections activated during the optimization process, using coplanar half arcs with couch structures included. Normal Tissue Objective (NTO) parameters were set manually to ensure a fast dose fall off beyond the PTV. To ensure a correct dose calculation it was crucial to take into consideration the multileaf collimator (MLC) characterization as well as the accuracy of the planning system for small fields [29]. The MLC was characterized in the treatment planning system following the recommendations by Saez et al [30]. Minimum jaw field size was set to 35 mm, while the output of smaller fields, conformed with MLC, was verified using EBT4 radiochromic films [31]. To reduce complexity of the plans the aperture shape controller was set to high strength and total MU were limited according to the prescribed dose per session in the optimization process. This ensured an acceptable dose distribution while avoiding unnecessary MLC modulation.

We analyzed the relationship between CTR and the relative differences between D98% (Gy) and D2% (Gy) on the PTV. Furthermore, Dmean was analyzed for the PTV-ITV area, where the differences are expected to be more appreciable due to density differences. For ease of interpretation we divided the sample in two groups, the first one with CTRs ranging from 0 and 0.33 (low CTR) and the second one with CTRs above 0.33 (mid-high CTR).

2.2. Evaluation of lung dose reduction after dose de-escalation

To evaluate the treatment plans with the least amount of variability, we reoptimized and recalculated with $AXB_{m,m}$ the dose distribution for the 40 lesions with a limited set of optimization parameters. The same physicist optimized the plans with the original dose prescription and with a dose reduction to the GGO component and following the same optimization procedure. For the standard approach, dose was normalized to ensure 100 % of the prescribed dose covered 95 % of the PTV. For the de-escalation case, dose was normalized to ensure 100 % of the prescribed dose covered 95 % of the solid PTV. The dose to the GGO component of the PTV (Fig. 1) was lowered as much as possible, but always granting that at least 100 % of the lower dose covered 95 % of the GGO PTV. Maximum doses were limited to 140 % of the prescribed dose. Other parameters were optimized following the RTOG 0236 trial protocol. The characteristics of the analysed lesions in terms of CTR, CTRv, lesion size and prescription are summarized in Table 1.

We analyzed the lung dose reduction in terms of the mean lung dose (Dmean) and the percentage of volume receiving 20 Gy (V20Gy), as they are associated with grade II or higher toxicities. We also analyzed the absolute volume of the lung receiving $V300Gy_{BED3}$, as it has recently been correlated with radiological toxicity [19]. Furthermore, for those patients with more than one lesion, we analyzed the same parameters considering the treatment of both lesions simultaneously.

We statistically analyzed the differences for Dmean, V20Gy and $V300Gy_{BED3}$ between the standard prescription and the de-escalation protocol using a paired *t*-test using RStudio software version 2022.07.2. We also analyzed the correlation between the lung dose

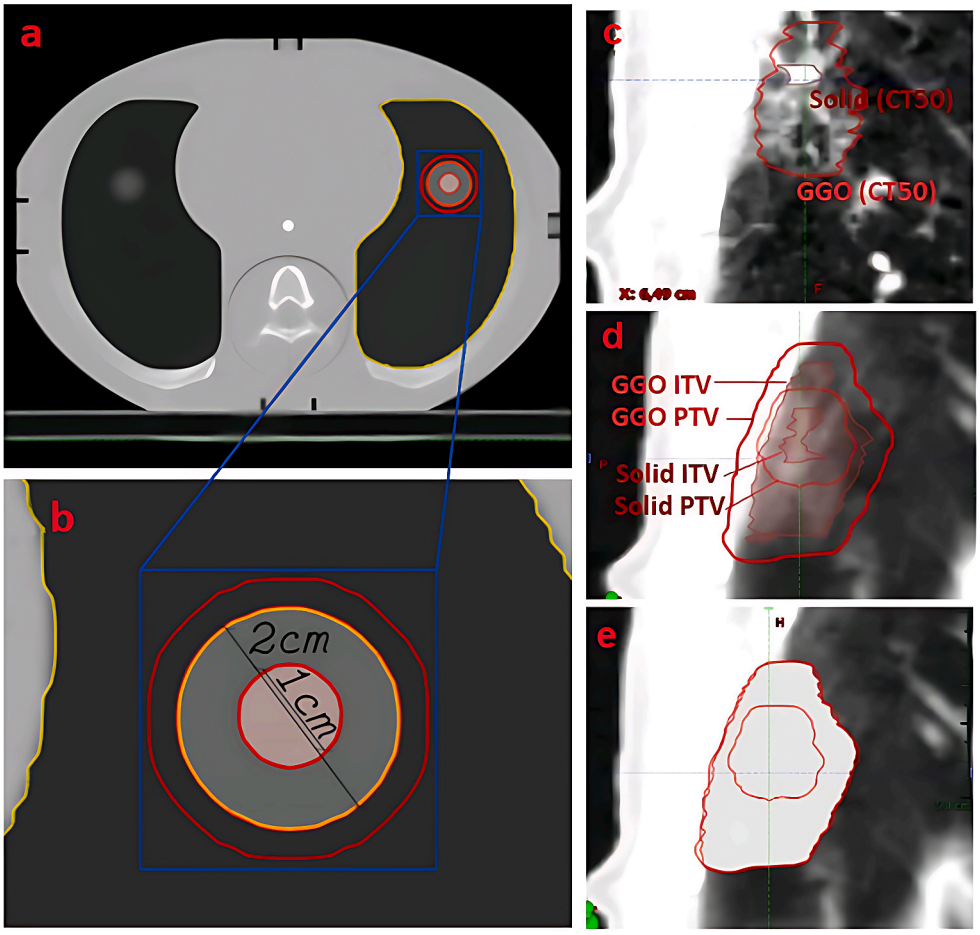

Fig. 1. Definition of target volumes. (a) Lung Phantom with a zoomed figure to a lesion corresponding to CTR of 0.5. Figure (c) is an example of the GTV volume delineation of a patient lesion on the 50 % expiration phase (CT50). The accumulated GTV was generated in the Average reconstruction of the 4DCT (d) to create the ITV. A 3 mm margin was added to generate the PTV. In Figure (e) we can see the structure set with the PTV area density and material overwritten to water to evaluate robustness.

reduction and the CTR and CTR_v using the Spearman's Ranks correlation coefficient.

2.3. Evaluation of dose distribution robustness

To evaluate the robustness of the treatment when optimizing with two dose levels with $AXB_{m,m}$, we used three datasets: Firstly, we used the plan optimized using AAA dose calculation algorithm with one dose level. Secondly, the same plan optimized using $AXB_{m,m}$ with one dose level and, finally, a plan optimized using $AXB_{m,m}$ with two dose levels (dose reduction to the GGO). These plans were optimized using the average CT scan of the 4DCT.

We then recalculated ($AXB_{m,m}$) with fixed MU these three plans to a new average CT with the PTV volume overridden (material and HU) to water (Fig. 1). When recalculated in water, possible fluence peaks in the area surrounding the ITV become apparent and comparison between algorithms is performed under the same dose transportation and deposit conditions. The analysis of these peaks allowed us to evaluate robustness of the plan against any motion of the GTV within the PTV region. To evaluate the magnitude of these fluence peaks, we compared the mean dose to the ITV with the dose to the ring between the ITV and the PTV (DmeanP-I/DmeanITV). Differences between the three scenarios were evaluated using a one-way ANOVA test.

3. Results

3.1. Evaluation of dose calculation accuracy as a function of GGO component

In the phantom case, we found relevant differences between the dose distributions calculated by the two algorithms in correlation with the CTR value. As shown in Fig. 2, the low CTR group (high GGO component) presented higher differences than the mid-high CTR group for the D2% parameter. While for the low CTR group the average difference between algorithms was 2 %, for the high CTR group this difference was reduced to 1 %. These differences were statistically significant ($p = 0.04$) and were also correlated with CTR for D98% ($p = 0.04$), going from an average difference of 2.5 % to 2 %.

In the clinical cases, the lesions led to PTVs with an equivalent sphere diameter ranging from 9.8 to 24.5 mm and CTRs from 0.00 to 0.90. Both variables were roughly normally distributed. Dose differences between both algorithms were found as previously reported in the literature. Differences in D2% were on average 1 % ranging from 0.5 % to 5.4 %. Differences in D98% between both algorithms were higher, with an average value of 6 % ranging from 0.5 % to a 20 %. In this case, however, neither the ITV scenario (Average CT) nor the gated scenario revealed any statistically significant difference between the two CTR groups.

3.2. Evaluation of lung dose reduction after dose de-escalation

The lung dose reduction obtained in terms of $V300Gy_{BED3}$, Dmean

Table 1
Summary of patient treatment characteristics, lesion volumes and CTR and lung dose, for the standard treatment and the dose de-escalation case.

	Average [min; max]	
PTV Volume (cm^3)	26 [4; 64]	
Sòlid PTV Volume (cm^3)	12 [0; 35]	
GGO PTV Volume (cm^3)	13 [2; 44]	
CTRv	0.52 [0; 0.93]	
CTR	0.69 [0; 0.97]	
	N	
Number of lesions	40	
3 @ 18 Gy	9	
5 @ 11 Gy	31	
Patients with 1 lesion	30	
3 @ 18 Gy	7	
5 @ 11 Gy	23	
Patients with two lesions	5	
3 @ 18 Gy	1	
5 @ 11 Gy	4	
Lung Dose Evaluation	**Standard**	**Dose de-escalation**
Dmean (Gy)	3.5 [1; 8]	3.1 [1; 7]
V20Gy (%)	4.3 [1; 13]	3.6 [1; 10]
V300GyBED3 (cm^3)	15.6 [2; 57]	7.1 [0; 29]
Multiple lesion patients		
Dmean (Gy)	5.0 [3,1; 7,1]	4.4 [2.5; 7]
V20Gy (%)	6.1 [5,0; 8]	5.4 [3.5; 7]
V300GyBED3 (cm^3)	21.5 [6,5; 34]	5.1 [0.7; 16]

and V20Gy can be seen in Fig. 3. An average reduction of 9 % (0.5 Gy) of Dmean was obtained. A reduction of V20Gy, from 3.6 % to 4.2 % and $V300Gy_{BED3}$ going from an average volume of 16 cm^3 to 7 cm^3 were also observed. Differences in all three variables were statistically significant ($p < 0.01$). When focusing the subgroup with a GGO volume above 20 cm^3, the reduction in Dmean and V20Gy increased to a 5.3 % and 8.5 % respectively and we observed an average $V300Gy_{BED3}$ reduction of 21 cm^3.

For $V300Gy_{BED3}$ the number of lesions with an absolute lung volume greater than 20 cm^3 went from 11 to 2 cases. The number of lesions with $V300Gy_{BED3} > 30$ cm^3 went from 4 to none.

Spearman's correlation between CTR or CTRv (Fig. 4) with the differences observed in lung doses ranged between 0.3 for V20Gy to 0.53 for $V300Gy_{BED3}$, indicating a low to moderate correlation ($p < 0.05$). The correlation was clearer when we analyzed the lung dose reduction in terms of the absolute volume of the GGO component of the lesion, ranging from a correlation of 0.56 for V20Gy to 0.78 for $V300Gy_{BED3}$ ($p < 0.05$). As it can also be seen in Fig. 4, the patients with GGO above 20 cm^3 all achieved a significant reduction in lung dose, with an average $V300Gy_{BED3}$ reduction of 21 cm^3, a reduction of Dmean of 0.5 % and a reduction in V20Gy of 1.1 %.

It is compelling to analyze the 5 patients with 2 lesions (Table 1). For these patients a mean lung dose reduction of 14 % (0.5 Gy) was obtained, with V20Gy going from 6 % to 5.4 %. The most significant reduction was obtained for $V300Gy_{BED3}$ with 3 out of 5 patients going from volumes above 20 cm^3 to all of them being below 20 cm^3, and an average reduction of 16 cm^3.

3.3. Dose distribution robustness

As it has been previously reported, we observed fluence peaks in the low-density area surrounding the PTV (Fig. 5). This effect was more evident when using $AXB_{m,m}$ during the optimization process and led to bigger fluence peaks compared to AAA ($p = 0.02$). When recalculated to water, the average dose for the region between the ITV and the PTV had an average dose of 0.98 for the AAA case compared to the ITV average dose. This value increased to an average of 1.015 for the $AXB_{m,m}$ case, showing a higher average dose on the area between the ITV and the PTV than within the ITV.

The analysis of the same parameters for the dose de-escalation case can be seen in Fig. 5. As it can be seen the fluence peaks were almost nonexistent (with an average value of 0.96 compared to the ITV dose value), similarly to the AAA-optimized scenario ($p > 0.05$) but clearly lower than the original $AXB_{m,m}$ optimization ($p < 0.01$).

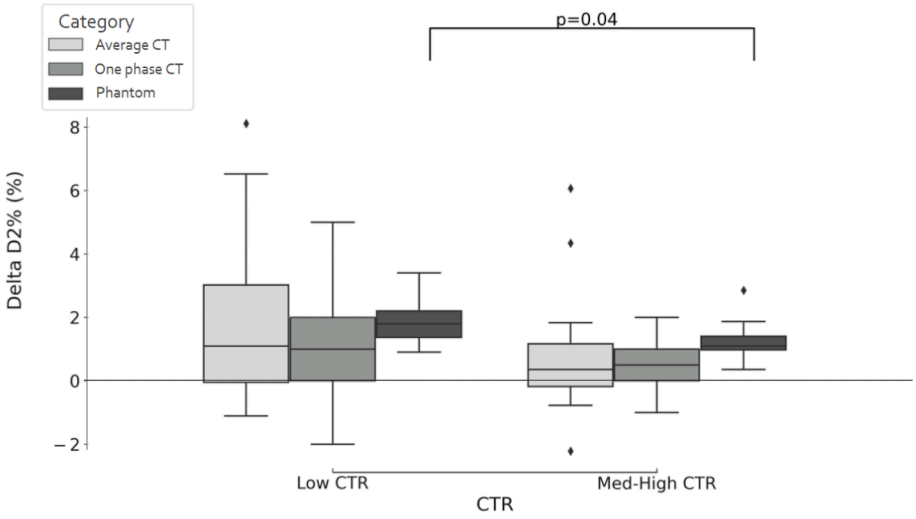

Fig. 2. Relative difference in the D2% (Gy) parameter between AAA and AXB for the different datasets. Low CTR corresponds to CTR < 0.33, while Med-High to CTR > 0.33. Differences are statistically significant only for the phantom case.

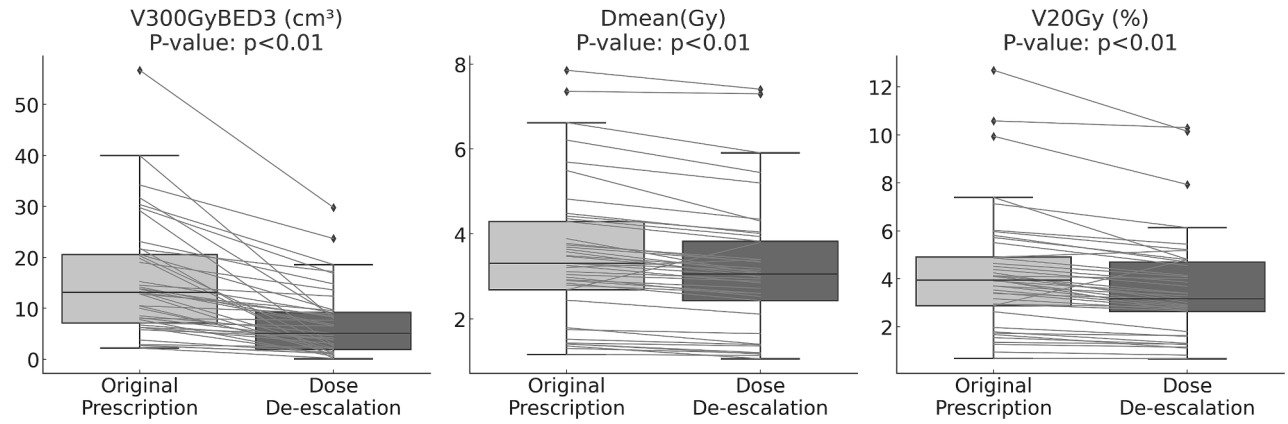

Fig. 3. Dose differences in the lung between the standard dose prescription and the dose de-escalation approach. Left: Reduction of V300GyBED3, with an average difference from 16 cm^3 to 7 cm^3. Center: Differences in lung Dmean, with an average reduction of 0.5 Gy. Right: V20Gy (%) showing a reduction from 4.2 % to 3.6 %.

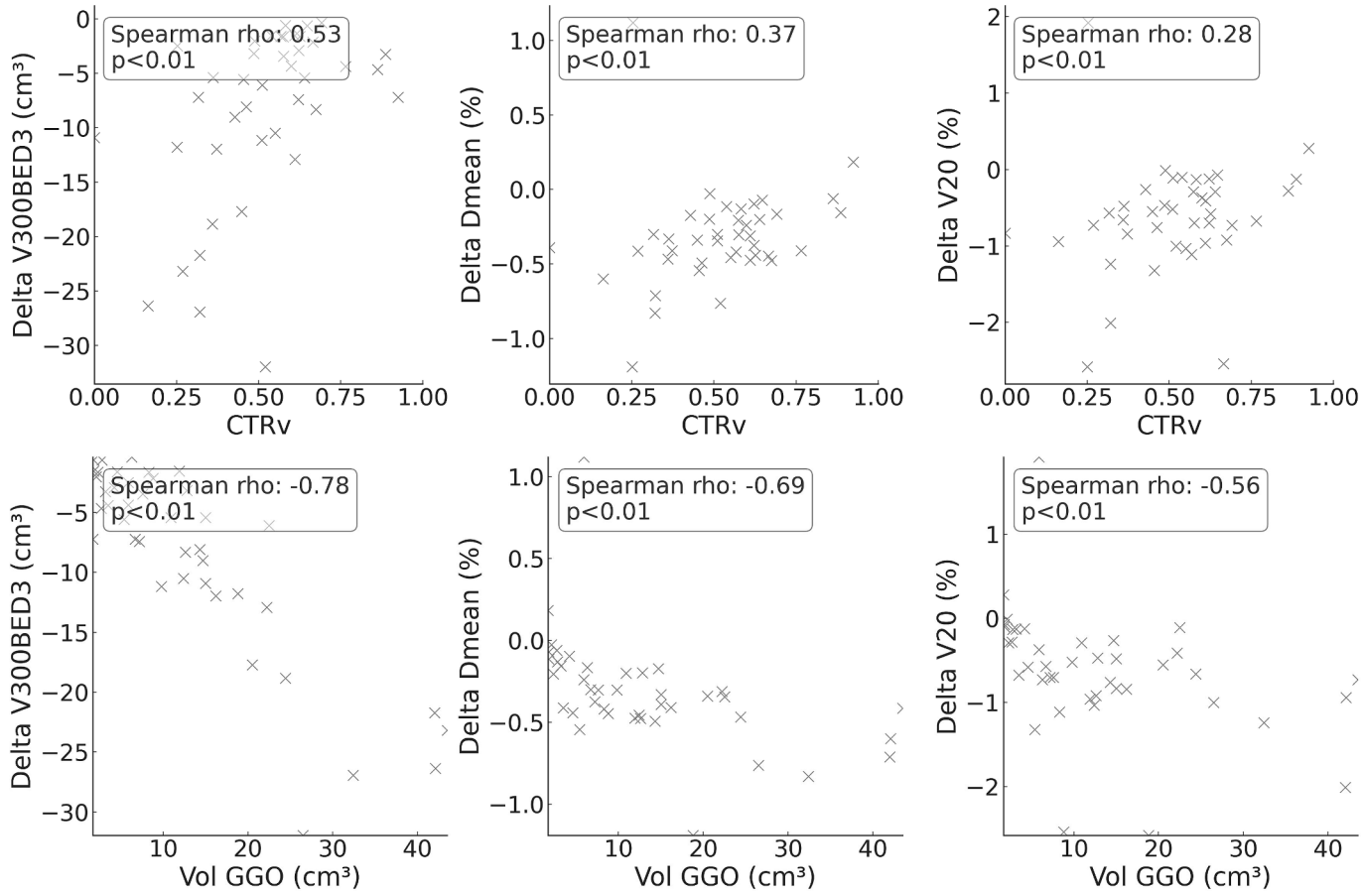

Fig. 4. Dose reduction in the lung between the standard dose prescription and the dose de-escalation approach in lung in terms of CTRv (top) or absolute Volume of the GGO PTV component (bottom). Dose reduction is analysed in terms of V300GyBED3 (Left), Dmean (centre) and V20Gy (%) (Right).

4. Discussion

In this study, we have analyzed the technical feasibility and potential benefit of a dose de-escalation strategy for the SABR treatment of lung lesions with GGO component. Regarding dose calculation accuracy, we have observed larger discrepancies when using type B calculation engines, such as AAA, for lower CTR values. These differences are less evident for blurrier borders between the solid and the GGO components, and even less significant when breathing motion is present. Although the observed differences between AAA and $AXB_{m,m}$ are similar in magnitude to the ones previously reported [23], extra care should be taken in SABR treatments involving GGO, especially for low CTR or when using gating strategies.

Dose de-escalation strategies have been successfully used previously in the context of SABR in the lung to prevent chest wall toxicities [17]. In our study, we have demonstrated that by de-escalating the dose in the GGO region, there is a systematic reduction of lung Dmean, V20, and $V300Gy_{BED3}$. Although these differences are small in some cases, they become relevant for lesions that contain a higher volume of GGO. It is for this group of patients that LC rates are expected to be higher [33]. From

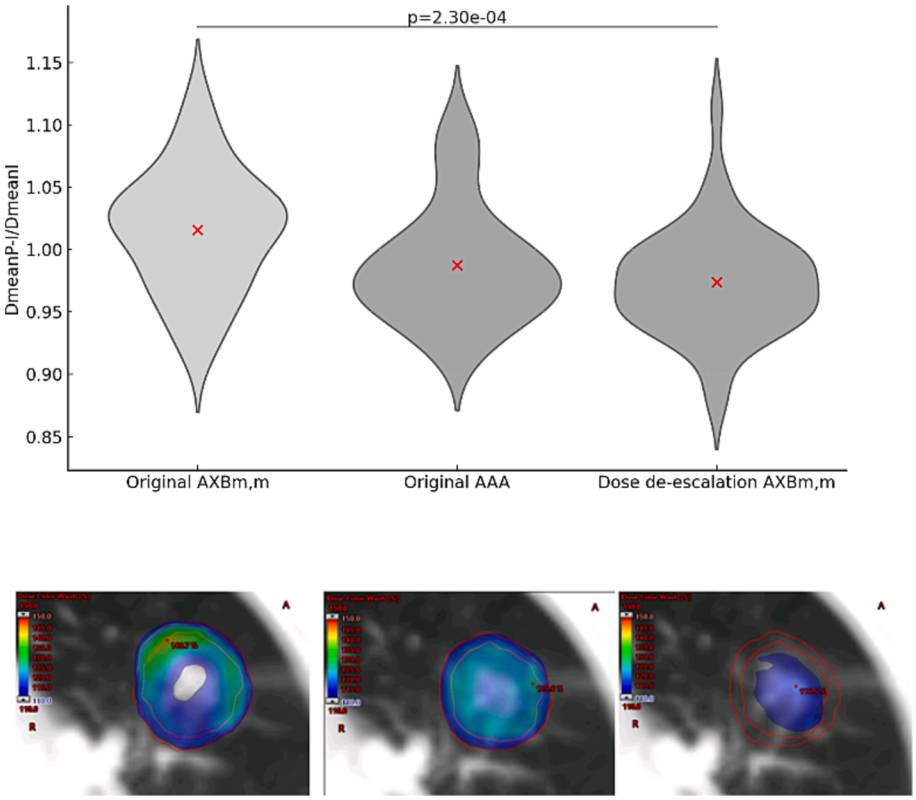

Fig. 5. Top: Robustness analysis in terms of Mean dose to the PTV –ITV area (MeanP-I) divided by mean dose to the ITV. Bottom: Dose distribution of one of the patients for the three cases of the top figure, in the same order. Colour wash levels are fixed for the three cases with the lower threshold at 110% of the prescribed dose and the upper threshold to the 150% of the prescribed dose.

the author's point of view, patients with CTR below 0.5 or absolute GGO volumes above 20 cm^3 would benefit from a dose de-escalation regime.

Finally, the lower dose in the GGO area, which is generally surrounding the solid lesion, provides a naturally more robust fluence, reducing the necessity to apply any strategy to mitigate fluence peaks. In contrast to the plans obtained when the dose distribution is forced to deliver high doses to less dense tissues, a dose de-escalation to the lesser dense tissue surrounding the solid nodule allows for more robust fluences.

This study, while providing insights into dose de-escalation strategies, has some limitations. The sample size was sufficient to derive some statistical conclusions. However, a more extensive study population, including more cases of very low CTR and high GGO volume, would provide a better understanding of the impact of the dose reduction. Furthermore, this study only evaluates the technical feasibility of the technique using Ecplise as optimization and calculation engines. The results observed in this study should not be directly assumed for other planning systems.

In conclusion, this work shows that a dose de-escalation strategy to lung cancer lesions with ground glass opacities is feasible in the context of SABR and dosimetrically advantageous. The use of a de-escalation scheme, maintaining the dose to the solid component of the lesion while reducing the dose to the GGO component, could lead to lower associated lung toxicities while maintaining local control. We believe that this work sets the basis for the design of a dose de-escalation clinical trial for GGO lesions, which should evaluate whether the reduction in lung dose observed here in silico translates to a reduction of lung toxicity in patient.

Declaration of competing interest

The authors declare that they have no known competing financial interests or personal relationships that could have appeared to influence the work reported in this paper.

REFERENCES

[1] Barriger RB, Forquer JA, Brabham JG, Andolino DL, Shapiro RH, Henderson MA, et al. A dose-volume analysis of radiation pneumonitis in non-small cell lung cancer patients treated with stereotactic body radiation therapy. Int J Radiat Oncol Biol Phys 2012;82(1):457–62. https://doi.org/10.1016/j.ijrobp.2010.08.056.

[2] Bongers EM, Botticella A, Palma DA, Haasbeek CJ, Warner A, Verbakel WF, et al. Predictive parameters of symptomatic radiation pneumonitis following stereotactic or hypofractionated radiotherapy delivered using volumetric modulated arcs. Radiother Oncol 2013 Oct;109(1):95–9. https://doi.org/10.1016/j.radonc.2013.10.011. Epub 2013 Oct 31 PMID: 24183862.

[3] Matsuo Y, Shibuya K, Nakamura M, Narabayashi M, Sakanaka K, Ueki N, et al. Dose-volume metrics associated with radiation pneumonitis after stereotactic body radiation therapy for lung cancer. Int J Radiat Oncol Biol Phys 2012 Jul 15;83(4):e545–9. https://doi.org/10.1016/j.ijrobp.2012.01.018. Epub 2012 Mar 19 PMID: 22436782.

[4] Saha A, Beasley M, Hatton N, Dickinson P, Franks K, Clarke K, et al. Clinical and dosimetric predictors of radiation pneumonitis in early-stage lung cancer treated with Stereotactic Ablative radiotherapy (SABR) - An analysis of UK's largest cohort of lung SABR patients. Radiother Oncol 2021 Mar;156:153–9. https://doi.org/10.1016/j.radonc.2020.12.015. Epub 2020 Dec 14 PMID: 33333139.

[5] Zhang Y, Fu F, Chen H. Management of Ground-Glass Opacities in the Lung Cancer Spectrum. Ann Thorac Surg 2020;110(6):1796–804. https://doi.org/10.1016/j.athoracsur.2020.04.094.

[6] Fu F, Zhang Y, Wen Z, Zheng D, Gao Z, Han H, et al. Distinct Prognostic Factors in Patients with Stage I Non-Small Cell Lung Cancer with Radiologic Part-Solid or Solid Lesions. J Thorac Oncol 2019 Dec;14(12):2133–42. https://doi.org/10.1016/j.jtho.2019.08.002. Epub 2019 Aug 19 PMID: 31437531.

[7] Ye T, Deng L, Wang S, Xiang J, Zhang Y, Hu H, et al. Lung Adenocarcinomas Manifesting as Radiological Part-Solid Nodules Define a Special Clinical Subtype. J Thorac Oncol 2019 Apr;14(4):617–27. https://doi.org/10.1016/j.jtho.2018.12.030. Epub 2019 Jan 17 PMID: 30659988.

[8] Chang B, Hwang JH, Choi YH, Chung MP, Kim H, Kwon OJ, et al. Natural history of pure ground-glass opacity lung nodules detected by low-dose CT scan. Chest 2013 Jan;143(1):172–8. https://doi.org/10.1378/chest.11-2501. PMID: 22797081.

[9] Li H, Wang Y, Chen Y, Zhong C, Fang W. Ground glass opacity resection extent assessment trial **(GREAT)**: A study protocol of multi-institutional, prospective, open-label, randomized phase III trial of minimally invasive segmentectomy versus

lobectomy for ground glass opacity (GGO)-containing early-stage invasive lung adenocarcinoma. Front Oncol 2023 Jan;19(13):1052796. https://doi.org/10.3389/fonc.2023.1052796. PMID: 36741022; PMCID: PMC9892852.

[10] National Lung Screening Trial Research Team; Aberle DR, Adams AM, Berg CD, Black WC, Clapp JD, Fagerstrom RM, et al. Reduced lung-cancer mortality with low-dose computed tomographic screening. N Engl J Med. 2011 Aug 4;365(5):395-409. 10.1056/NEJMoa1102873. Epub 2011 Jun 29. PMID: 21714641; PMCID: PMC4356534.

[11] Travis WD, Brambilla E, Noguchi M, Nicholson AG, Geisinger KR, Yatabe Y, et al. International association for the study of lung cancer/american thoracic society/european respiratory society international multidisciplinary classification of lung adenocarcinoma. J Thorac Oncol 2011 Feb;6(2):244–85. https://doi.org/10.1097/JTO.0b013e318206a221. PMID: 21252716; PMCID: PMC4513953.

[12] Klement RJ, Sonke JJ, Allgäuer M, Andratschke N, Appold S, Belderbos J, et al. Correlating Dose Variables with Local Tumor Control in Stereotactic Body Radiation Therapy for Early-Stage Non-Small Cell Lung Cancer: A Modeling Study on 1500 Individual Treatments. Int J Radiat Oncol Biol Phys 2020 Jul 1;107(3):579–86. https://doi.org/10.1016/j.ijrobp.2020.03.005. Epub 2020 Mar 15 PMID: 32188579.

[13] Huang BT, Lu JY, Lin PX, Chen JZ, Li DR, Chen CZ. Radiobiological modeling analysis of the optimal fraction scheme in patients with peripheral non-small cell lung cancer undergoing stereotactic body radiotherapy. Sci Rep 2015 Dec;11(5):18010. https://doi.org/10.1038/srep18010. PMID: 26657569; PMCID: PMC4676016.

[14] Woody NM, Videtic GM, Stephans KL, Djemil T, Kim Y, Xia P. Predicting chest wall pain from lung stereotactic body radiotherapy for different fractionation schemes. Int J Radiat Oncol Biol Phys 2012 May 1;83(1):427–34. https://doi.org/10.1016/j.ijrobp.2011.06.1971. Epub 2011 Dec 23 PMID: 22197087.

[15] Zhang J, Yang F, Li B, Li H, Liu J, Huang W, et al. Which is the optimal biologically effective dose of stereotactic body radiotherapy for Stage I non-small-cell lung cancer? A meta-analysis. Int J Radiat Oncol Biol Phys 2011 Nov 15;81(4):e305–16. https://doi.org/10.1016/j.ijrobp.2011.04.034. Epub 2011 Jun 12 PMID: 21658853.

[16] Bradley JD, Hope A, El Naqa I, Apte A, Lindsay PE, Bosch W, et al. A nomogram to predict radiation pneumonitis, derived from a combined analysis of RTOG 9311 and institutional data. Int J Radiat Oncol Biol Phys. 2007 Nov 15;69(4):985-92. 10.1016/j.ijrobp.2007.04.077. Epub 2007 Aug 6. PMID: 17689035; PMCID: PMC2196217.

[17] Ladbury CJ, Sampath S. Lung stereotactic body radiation therapy using simultaneous integrated BED-escalation for peripherally located non-small cell lung cancer. J Radiosurg SBRT. 2022;8(3):181-187. PMID: 36861004; PMCID: PMC9970741.

[18] Kenamond MC, Pokhrel D, Visak J, McGarry RC. Escalating Tumor Dose via Simultaneous Integrated Boost (SIB) Stereotactic Body Radiation Therapy (SBRT) for Large (> 5 cm) Lung Masses. Int J Radiat Oncol Biol Phys 2021;111(3, Suppl). https://doi.org/10.1016/j.ijrobp.2021.07.317.

[19] Cases C, Benegas M, Sánchez M, Vollmer I, Casas F, Gomà C, et al. Biological equivalent dose is associated with radiological toxicity after lung stereotactic ablative radiation therapy. Radiother Oncol 2023;183:109552. https://doi.org/10.1016/j.radonc.2023.109552.

[20] Palma DA, Olson R, Harrow S, Gaede S, Louie AV, Haasbeek C, et al. Stereotactic Ablative Radiotherapy for the Comprehensive Treatment of Oligometastatic Cancers: Long-Term Results of the SABR-COMET Phase II Randomized Trial. J Clin Oncol. 2020 Sep 1;38(25):2830-2838. 10.1200/JCO.20.00818. Epub 2020 Jun 2. PMID: 32484754; PMCID: PMC7460150.

[21] Asamura H, Hishida T, Suzuki K, Koike T, Nakamura K, Kusumoto M, et al. Japan Clinical Oncology Group Lung Cancer Surgical Study Group. Radiographically determined noninvasive adenocarcinoma of the lung: survival outcomes of Japan Clinical Oncology Group 0201. J Thorac Cardiovasc Surg 2013 Jul;146(1):24–30. https://doi.org/10.1016/j.jtcvs.2012.12.047. Epub 2013 Feb 8. PMID: 23398645.

[22] Chetty IJ, Devpura S, Liu D, Chen D, Li H, Wen NW, et al. Correlation of dose computed using different algorithms with local control following stereotactic ablative radiotherapy (SABR)-based treatment of non-small-cell lung cancer. Radiother Oncol 2013 Dec;109(3):498–504. https://doi.org/10.1016/j.radonc.2013.10.012. Epub 2013 Nov 11 PMID: 24231237.

[23] Ojala JJ, Kapanen MK, Hyödynmaa SJ, Wigren TK, Pitkänen MA. Performance of dose calculation algorithms from three generations in lung SBRT: comparison with full Monte Carlo-based dose distributions. J Appl Clin Med Phys 2014 Mar 6;15(2):4662. https://doi.org/10.1120/jacmp.v15i2.4662. PMID: 24710454; PMCID: PMC5875463.

[24] Fogliata A, Cozzi L. Dose calculation algorithm accuracy for small fields in non-homogeneous media: The lung SBRT case. Phys Med 2017;44:157–62. https://doi.org/10.1016/j.ejmp.2016.11.104.

[25] Healy GEA, Marsh SH, Cousins AT. The dosimetric effect of electron density overrides in 3DCRT Lung SBRT for a range of lung tumor dimensions. J Appl Clin Med Phys 2018;19(6):79–87. https://doi.org/10.1002/acm2.12446.

[26] Wiant D, Vanderstraeten C, Maurer J, Pursley J, Terrell J, Sintay BJ. On the validity of density overrides for VMAT lung SBRT planning. Med Phys 2014 Aug;41(8):081707. https://doi.org/10.1118/1.4887778. PMID: 25086517.

[27] Liang X, Zheng D, Mamalui-Hunter M, Flampouri S, Hoppe BS, Mendenhall N, et al. ITV-Based Robust Optimization for VMAT Planning of Stereotactic Body Radiation Therapy of Lung Cancer. Pract Radiat Oncol 2019 Jan;9(1):38–48. https://doi.org/10.1016/j.prro.2018.08.005. Epub 2018 Aug 20 PMID: 30138747.

[28] Xi J, Yin J, Liang J, Zhan C, Jiang W, Lin Z, et al. Prognostic Impact of Radiological Consolidation Tumor Ratio in Clinical Stage IA Pulmonary Ground Glass Opacities. Front Oncol 2021 Apr;12(11):616149. https://doi.org/10.3389/fonc.2021.616149. PMID: 33912445; PMCID: PMC8072116.

[29] Van Esch A, Kulmala A, Rochford R, Kauppinen J, Harju A. Testing of an enhanced leaf model for improved dose calculation in a commercial treatment planning system. Med Phys 2022 Dec;49(12):7754–65. https://doi.org/10.1002/mp.16019. Epub 2022 Oct 17 PMID: 36190516.

[30] Saez J, Hernandez V, Goossens J, De Kerf G, Verellen D. A novel procedure for determining the optimal MLC configuration parameters in treatment planning systems based on measurements with a Farmer chamber. Phys Med Biol 2020 Jul 27;65(15):155006. https://doi.org/10.1088/1361-6560/ab8cd5. PMID: 32330917.

[31] Öllers MC, Swinnen ACC, Verhaegen F. Acuros® dose verification of ultrasmall lung lesions with EBT-XD film in a homogeneous and heterogeneous anthropomorphic phantom setup. Med Phys 2020 Nov;47(11):5829–37. https://doi.org/10.1002/mp.14485. Epub 2020 Oct 7 PMID: 32970849.

[32] Bainbridge H, Dunlop A, McQuaid D, Gulliford S, Gunapala R, Ahmed M, et al. A Comparison of Isotoxic Dose-escalated Radiotherapy in Lung Cancer with Moderate Deep Inspiration Breath Hold, Mid-ventilation and Internal Target Volume Techniques. Clin Oncol (R Coll Radiol) 2022 Mar;34(3):151–9. https://doi.org/10.1016/j.clon.2021.08.012. Epub 2021 Sep 7 PMID: 34503896.

[33] Liang X, Zhang C, Ye X. Overdiagnosis and overtreatment of ground-glass nodule-like lung cancer. Asia Pac J Clin Oncol. 2024 Jan 4. 10.1111/ajco.14042. Epub ahead of print. PMID: 38178320.